Applied Catalysis B: Environmental 140–141 (2013) 671–679

Contents lists available at SciVerse ScienceDirect

Applied Catalysis B: Environmental

journal homepage: www.elsevier.com/locate/apcatb

Green preparation of transition metal oxide catalysts using supercritical CO_2 anti-solvent precipitation for the total oxidation of propane

Raimon P. Marin, Simon A. Kondrat, Rebecca K. Pinnell, Thomas E. Davies, Stan Golunski, Jonathan K. Bartley, Graham J. Hutchings, Stuart H. Taylor*

Cardiff Catalysis Institute, School of Chemistry, Cardiff University, Main Building, Park Place, Cardiff, CF10 3AT, UK

ARTICLE INFO

Article history:
Received 1 March 2013
Received in revised form 25 April 2013
Accepted 30 April 2013
Available online 8 May 2013

Keywords:
Propane
Total oxidation
Supercritical anti-solvent precipitation
Metal oxides
Cobalt oxide

ABSTRACT

A series of metal oxide catalysts, including Fe_3O_4, NiO, CuO and Co_3O_4, have been prepared by supercritical anti-solvent precipitation and evaluated for the total oxidation of propane. Co_3O_4 was found to be the most active catalyst and our studies have focussed on this oxide. The addition of water as co-solvent in the supercritical anti-solvent preparation was investigated. Powder X-ray diffraction and infrared spectroscopy indicated that the addition of water promoted the formation of carbonate species in the catalyst precursors. The formation of the catalysts from the precursor were optimised by investigating the thermal treatment conditions, by studying variables including time, temperature and atmosphere. The optimal conditions for catalyst preparation required precursor precipitation containing 10 vol% water co-solvent followed by a 2 h calcination at 250 °C. These conditions produced Co_3O_4 with high surface areas (>100 $m^2\ g^{-1}$), which were very active catalysts producing 50% propane conversion at 175 °C.

1. Introduction

The challenge to control atmospheric emissions from a wide range of sources is of great importance, with increasingly stringent legislation being introduced to limit their release in an attempt to abate their detrimental environmental properties. In particular, volatile organic compounds (VOCs) are recognised as major atmospheric pollutants. VOCs are involved in ground level ozone formation [1], ozone depletion [2] and the greenhouse effect [3]. Amongst compounds classified as VOCs, linear short chain alkanes are among the most difficult to eliminate [4]. Therefore, much research has been dedicated to their removal, with catalytic total oxidation being recognised as one of the most efficient methods, with supported platinum and palladium catalysts commonly used commercially.

Propane oxidation has been widely used as a model reaction to study the oxidation of short chain VOCs. A number of transition metal oxides have shown promising activity for propane deep oxidation, with Co_3O_4 and Mn_2O_3 being particularly active [5–8]. Mixed metal oxide systems, such as $NiMnO_x$, $FeMnO_x$ and $CuMnO_x$, have also been investigated, with improvements in activity reported compared to the relevant single metal oxides [8–10]. Solsona et al. observed that co-precipitated $CuMnO_x$ was more active than supported palladium catalysts, and activity was further improved by the incorporation of gold nanoparticles into the $CuMnO_x$ structure [11]. Moreover, the incorporation of gold enhanced catalyst stability over 24 h at 250 °C. Although some mixed metal oxides are very active and warrant further investigation, nanocrystalline Co_3O_4 has shown higher activity, with total oxidation at 200 °C [6]. Therefore much interest remains focussed on this single metal oxide catalyst.

The preparation method of nanocrystalline Co_3O_4 has been found to be highly influential for propane total oxidation activity. Several preparation techniques have been investigated, including mechano-chemical synthesis [5–7,12], sol gel synthesis [13], co-precipitation [13] and hard templating [14]. Mechano-chemical synthesis using cobalt nitrate and ammonium carbonate produced very active nanocrystalline Co_3O_4 catalysts, with propane conversion reported at temperatures as low as 40 °C [5–7]. Solsona et al. [6,7] produced a very active nanocrystalline Co_3O_4 catalyst using this technique with high surface area (160 $m^2\ g^{-1}$). It was observed that these high surface area cobalt oxides are more reducible, with low Co—O bond strengths, which suggests a high concentration of oxygen defect sites. Liu et al. also investigated mechano-chemical synthesis and proposed that lattice strain in nanocrystalline Co_3O_4 was responsible for oxygen defect sites, and consequently the high activity [12]. The importance of a disordered structure was confirmed by Garcia et al. who prepared highly ordered and high

* Corresponding author. Tel.: +44 0 29 20 87 4062.
E-mail address: taylorsh@cardiff.ac.uk (S.H. Taylor).

0926-3373/$ – see front matter © 2013 Elsevier B.V. All rights reserved.
http://dx.doi.org/10.1016/j.apcatb.2013.04.076

surface area (177 $m^2 g^{-1}$) Co_3O_4 by nanocasting using a mesoporous silica KIT-6 framework [14]. It was observed that partially ordered cobalt oxide was more active than the highly ordered oxides. The activity was attributed to the relatively high concentration of reactive oxygen defects which correlated with the measured concentration of Co^{2+} on the surface.

Amorphous or poorly crystalline high surface area metal oxides have been synthesised previously using supercritical CO_2 anti-solvent (SAS) precipitation. There has been extensive research into SAS for the synthesis of semiconductors, polymers, pharmaceuticals and explosives [15–20]. With respect to use for heterogeneous catalyst synthesis, SAS produced materials have been investigated as supports for noble metals and as catalysts themselves. Medziak et al. [21] reported gold and palladium impregnated onto SAS precipitated CeO_2 as catalysts for benzyl alcohol oxidation, while Tang et al. [22] supported gold on SAS precipitated CeO_2 and TiO_2 to show high catalytic activity for CO oxidation. Scanning transmission electron microscopy (STEM) analysis of these catalysts showed exceptionally high dispersion of the metals, which was attributed to the defective nature of the SAS prepared supports. Amorphous vanadium phosphate catalysts have also been successfully prepared for n-butane oxidation to maleic anhydride, demonstrating high intrinsic activity and no induction period, which is usually observed when conventionally prepared catalysts are used [23,24]. Similarly, hopcalite ($CuMnO_x$) prepared by SAS had very high activity per unit area [25]. This high activity was attributed to the homogeneous distribution of metals and highly defective structure that was facilitated by the high nucleation rates provided by SAS precipitation. However, hopcalite surface areas from SAS precipitation using DMSO as solvent were found to be considerably lower, at *ca.* 10 $m^2 g^{-1}$, when compared to surface areas of conventionally prepared Hopcalite (90–100 $m^2 g^{-1}$) [26]. This resulted in the catalyst mass normalised CO conversion (which is a crucial factor for hopcalite catalysts) being lower for the SAS precipitated materials. However, the surface area of hopcalite was found to increase by adding water as a co-solvent during the SAS precipitation, which enabled materials with surface areas of up to 175 $m^2 g^{-1}$ to be obtained [27].

SAS precipitation, in addition to producing novel heterogeneous catalysts with advantageous properties, provides a preparation route which is in accordance with the principles of green chemistry [28,29]. The process avoids the use of metal nitrate salts, which result in environmentally damaging nitrate effluent streams, by preferentially using acetate salts [18,27]. The use of a supercritical fluid as an anti-solvent allows for easy separation of the solvents and recovery of the supercritical fluid [30]. In addition supercritical CO_2 has a low cost, low toxicity, relatively mild operational conditions and can be easily recycled [30,31].

The current study investigates the preparation of a range of transition metal oxide catalysts, for propane total oxidation, using supercritical CO_2 anti-solvent precipitation. This is the first time these catalysts have been prepared using a supercritical method, and their performance evaluated. After initial catalyst screening of the metal oxides, Co_3O_4 was found to be the most promising material. The synthesis parameters for this catalyst were investigated in more detail, in order to evaluate the influence of addition of water as a co-solvent, calcination time and temperature on catalyst activity.

2. Experimental

2.1. Catalyst preparation

Various metal acetate salts (Sigma–Aldrich), shown in Table 1, were dissolved in methanol (reagent grade, Fischer Scientific) at a concentration of 7 mg ml^{-1}. SAS experiments were performed using apparatus manufactured by Separex, according to the methodology described previously [23]. CO_2 (BOC) was pumped through the system *via* the outer part of a coaxial nozzle at 120 bar, 40 °C at a rate of 9 kg h^{-1}. The metal salt solution was co-currently pumped through the inner nozzle, using a HPLC pump at a rate of 3.75 ml min^{-1}. The resulting precipitate was recovered on a frit, while the CO_2-solvent mixture passed down stream, where the pressure was decreased to separate the two components. Precipitation was carried out for 90 min followed by a purge of the system with CO_2 under the reaction conditions. The system was then de-pressurised and the dry powder collected and calcined in static air at 250–400 °C for 2–5 h.

The effect of water addition during the precipitation of cobalt (II) acetate tetrahydrate ($Co(CH_3COO)_2{\cdot}4H_2O$) was investigated by adding between 0 and 15 vol% water co-solvent to the methanol solution. SAS precipitation was performed under the same conditions as described above. The most active catalyst from the initial screening was then subjected to different calcination temperatures from 250 to 400 °C. Several catalysts were used to benchmark the activity of the SAS catalysts. These included commercial Co_3O_4 (Sigma–Aldrich) and Co_3O_4 prepared from cobalt(II) acetate tetrahydrate (Sigma–Aldrich) by calcination at 400 °C for 5 h with a ramp rate of 5 °C min^{-1}. Finally the activity for propane total oxidation for the optimised SAS Co_3O_4 catalyst was compared to a commercial 5 wt% Pt/Al_2O_3 catalyst.

2.2. Catalyst characterisation

Surface areas were determined by multi-point N_2 adsorption at -196 °C using a Micromeretics Gemini 2360 according to the Brunauer–Emmett–Teller method. Powder X-ray diffraction (XRD) was performed using a PANalytical X'Pert Pro diffractometer with a monochromatic Cu Kα source ($\lambda = 0.154$ nm) operated at 40 kV and 40 mA. The scans were recorded over the range 10–80° 2θ using a step size of 0.016° and a scan step time of 55 seconds. Fourier transform infra-red (FT-IR) analysis was carried out using a Jasco FT/IR 660 Plus spectrometer in transmission mode over a range of 400–4000 cm^{-1}. Catalysts were supported in a pressed KBr disc. Scanning electron microscopy (SEM) was performed by dispersing the catalyst on an adhesive carbon disc, mounted on a 12.5 mm aluminium stub. Analysis was performed using a Carl Zeiss Evo 40 microscope, operated at 5–20 kV and 50–2000 pA. Thermal gravimetric analysis (TGA) was performed using a SETARAM Labsys thermogravimetric analyser. Temperature programmed reduction (TPR) was performed under 10% H_2/Ar to elucidate catalyst reducibility using a ChemBet 3000 instrument from 50 °C to 900 °C.

2.3. Catalyst testing

Catalysts were tested for propane total oxidation at ambient pressure under steady state conditions in a laboratory microreactor. 0.5 ml of catalyst were packed inside a stainless steel tube and placed inside a tubular furnace. The mass of SAS precipitated catalysts used was between 0.08 and 0.13 g, whilst the significantly denser standard catalysts used for comparison required *ca.* 0.2 g being used. A reaction gas mixture consisting of 0.5 vol% propane balanced with synthetic air (20 vol% O2/He) was flowed over the catalyst bed at 50 ml min^{-1} (GHSV of 6000 h^{-1}) controlled by MKS mass flow controllers. The product stream was analysed using an on-line Varian 3800 gas chromatograph equipped with thermal conductivity and flame ionisation detectors. Activity was determined using incremental temperature steps. The catalyst was maintained at each temperature until steady state was achieved and three analyses were made and the data averaged. The catalyst was then increased to the next temperature and the process

Table 1
Surface areas, crystallite sizes and surface area normalised rates of propane oxidation of various SAS precipitates after calcination.

Material	Surface area ($m^2\ g^{-1}$)		Crystallite size[a] (nm)	Phase of calcined material	Rate[b] (mmol $min^{-1}\ m^{-2}$)
	Precipitated	Calcined			
$Fe(CH_3COO)_2$	105	71	9	Fe_3O_4	6.31×10^{-4}
$Cu(CH_3COO)_2{\cdot}H_2O$	72	2	49	CuO	3.36×10^{-2}
$Co(CH_3COO)_2{\cdot}4H_2O$	112	16	43	Co_3O_4	3.50×10^{-2}
$Ni(CH_3COO)_2{\cdot}4H_2O$	16	26	10	NiO	2.58×10^{-3}

[a] Crystallite size calculated using Scherrer equation.
[b] Rate of propane oxidation at 300 °C normalised for catalyst surface area.

repeated. Carbon balances were typically found to be between 95 and 105%.

3. Results and discussion

3.1. Catalyst screening of selected transition metal oxides

X-ray diffraction from the precipitated catalyst precursors indicated that the materials were amorphous (data not shown). This is markedly different to the highly crystalline acetate salts before SAS precipitation. The formation of amorphous precursors was attributed to the fast nucleation rate achieved by SAS precipitation, which has been observed for previous SAS precipitation studies [32,33]. The surface areas of most of the metal precipitates were relatively large, with values between 70 and 110 $m^2\ g^{-1}$ (Table 1), and these are indicative of the high nucleation rates achieved by SAS precipitation. However, the nickel precipitated material had a relatively low surface area of 16 $m^2\ g^{-1}$ (Table 1). FT-IR spectroscopy of the SAS-precipitated materials (Fig. 1) showed the symmetric and asymmetric COO^- bands characteristic of acetate salts at 1568 and 1420 cm^{-1}. This demonstrates that the acetate salt is retained in the precipitation process, as previously observed for SAS precipitation [34]. The nickel and cobalt precipitated materials also showed bands at 1500 and 840 cm^{-1} which are associated with the presence of CO_3^{2-}. The formation of metal carbonate compounds by SAS precipitation in the presence of water has previously been ascribed to the reaction with carbonic acid formed during the precipitation process [27]. High levels of co-ordinated water in the Ni and Co acetate complexes (salts were tetrahydrated) was considered to be sufficient to partially form carbonate species *via* the same mechanism. The significant intensity of carbonate bands, relative to acetate, in the nickel sample could signify considerable amounts of metal carbonate formation and explain the low surface area obtained for this precursor.

XRD analysis of the catalysts after calcination under static air at 400 °C showed that the precipitated catalyst precursors were transformed into their corresponding metal oxides (Fig. 2 and Table 1). A direct trend between metal oxide crystallite size, calculated from the Scherrer equation and surface area was observed, with high areas correlating with a small crystallite size (Table 1). The surface area of SAS processed acetate materials have been previously observed to decrease after calcination [25]. This is due to the exothermic nature of acetate decomposition facilitating the sintering and collapse of the precursor structure [25,35]. However, for the nickel oxide catalyst the surface area slightly increased after calcination, which is attributed to the presence of carbonate in the precursor. It is known that the decomposition of metal carbonates, to form the corresponding oxides, results in preservation, or even an increase, of surface area due to the endothermic nature of the decomposition [36].

TPR profiles of the metal oxide catalysts are shown in Fig. 3. For cobalt oxide the expected reduction profile reported in the literature was observed, with Co_3O_4 reducing to CoO at *ca.* 295 °C, and CoO to Co metal at *ca.* 345 °C [37]. The three reduction steps for NiO have been observed previously and attributed to the loss of non-stoichiometric oxygen from Ni^{3+} to Ni^{2+} at *ca.* 305 °C, the reduction of small particles of nickel oxide to nickel metal at *ca.* 325 °C and the reduction of larger NiO particles at *ca.* 345 °C [38]. The Fe_3O_4 catalyst also presented the expected reduction profile, with Fe_3O_4 to FeO occurring at *ca.* 305 °C with further reduction to Fe at *ca.* 485 °C [39]. The SAS CuO catalyst presented one characteristic reduction peak (CuO to Cu) at *ca.* 255 °C.

The metal oxides were tested for propane total oxidation (Fig. 4). For all catalysts trace amounts of propene were observed at low

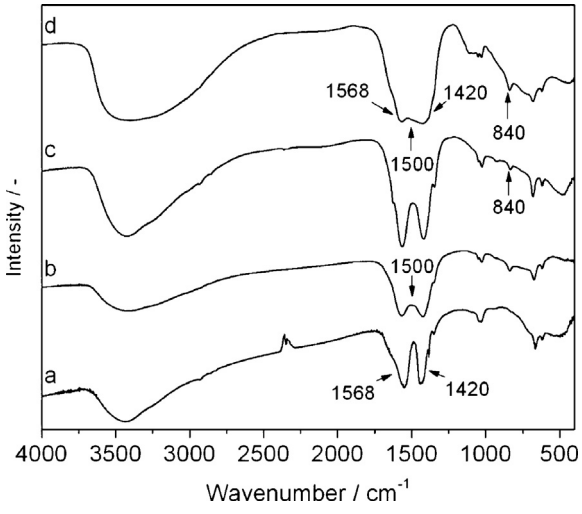

Fig. 1. FT-IR spectra of SAS metal precipitates: (a) iron precipitate, (b) cobalt precipitate, (c) nickel precipitate, (d) copper precipitate. Arrows indicate characteristic acetate salt carbonyl bands.

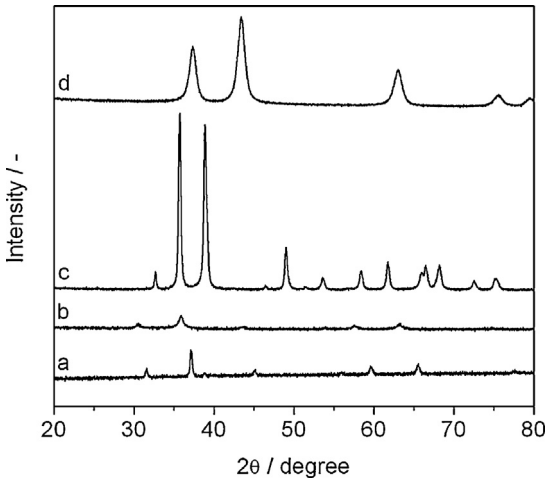

Fig. 2. XRD of SAS prepared precipitates calcined at 400 °C under static air for 5 h: (a) Fe_3O_4, (b) Co_3O_4, (c) NiO, and (d) CuO.

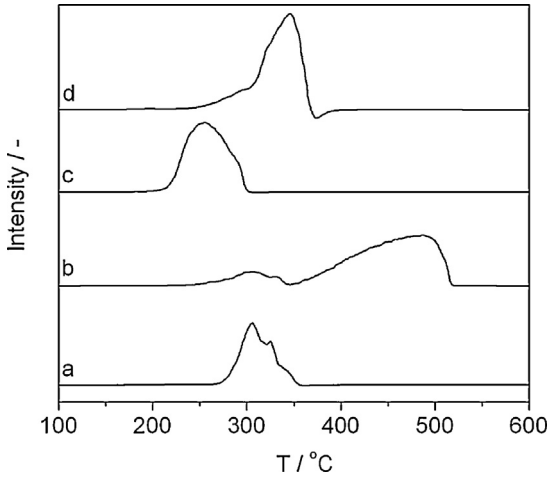

Fig. 3. TPR of metal oxides prepared from SAS precipitates: (a) Fe_3O_4, (b) Co_3O_4, (c) NiO, and (d) CuO.

conversions, which is consistent with previous observations [5]. The Co_3O_4 catalyst was observed to have T_{10} and T_{50} values (required temperature for 10 and 50% conversion) of 210 and 260 °C. The Fe_3O_4 and CuO catalysts had T_{10} conversions at around 300 °C, with T_{50} values being around 375–400 °C. Interestingly the NiO catalyst had a low T_{10} value of 210 °C but conversion increased slowly with increasing temperature and T_{50} was not reached. Full combustion of propane with the Co_3O_4 catalyst was achieved by 300 °C. The remaining CuO, Fe_3O_4 and NiO materials did not completely oxidise propane even at 400 °C. The activity of the simple metal oxides was also compared once the propane oxidation rate was normalised for surface area (Table 1). The rate was greatest for Co_3O_4, followed closely by CuO, although this was mainly due to the influence of the very low surface area of the CuO catalyst. Fe_3O_4 demonstrated a much lower normalised rate due to the considerably higher surface area of this catalyst.

The performance observed for the SAS precipitated materials show a similar trend to those observed for the corresponding metal oxides prepared by conventional routes [7–9]. From the initial screening of the SAS precipitated materials Co_3O_4 was identified as the most active catalyst. It was noted that the Co_3O_4 prepared using this methodology had a similar catalytic activity and reduction profile to previously reported Co_3O_4 catalysts with similar

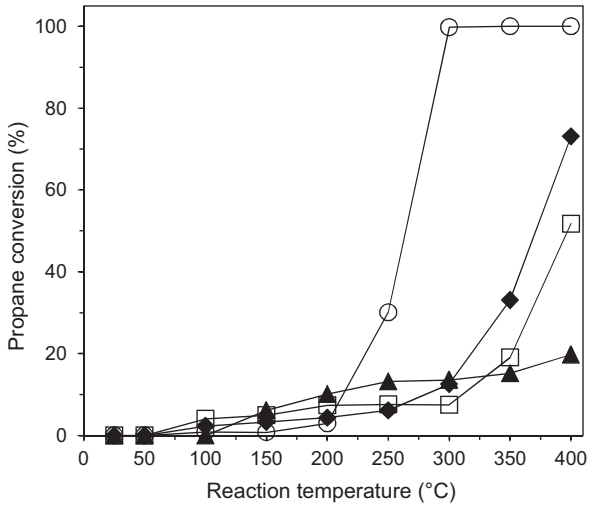

Fig. 4. Propane conversion as a function of temperature over various SAS prepared metal oxides: (□) Fe_3O_4; (○) Co_3O_4; (▲) NiO; (♦) CuO.

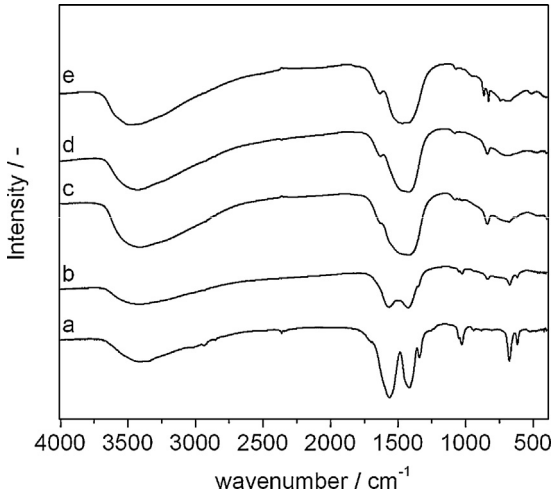

Fig. 5. FT-IR spectra of cobalt SAS precipitates with different water co-solvent addition, commercial cobalt acetate included for comparison: (a) commercial cobalt(II) acetate tetrahydrate, (b) 0 vol% water SAS, (c) 5 vol% water SAS, (d) 10 vol% water SAS, (e) 15 vol% water SAS.

surface areas [7]. Although surface area does not always directly correlate with catalytic activity, a higher surface area does offer the possibility of a higher number of active sites. Co_3O_4 catalysts have been extensively investigated in the literature, with optimisation by mechano-chemical preparation providing a precedent for increasing activity by increasing catalyst surface area. Hence, this led us to a more detailed investigation of the SAS precipitation of Co_3O_4.

3.2. The effect of water addition on the SAS precipitation of cobalt acetate

The addition of water to the metal acetate solution has been shown to change the SAS precipitation mechanism, and consequently the nature of the material prepared. Increasing water content resulted in the formation of metal carbonates instead of metal acetates which had a beneficial effect on the final surface area of the metal oxide [27]. Hence, in the present study the addition of 5, 10 and 15 vol% water to the initial cobalt acetate solution in methanol was investigated.

FT-IR analyses of the SAS precipitated precursors (Fig. 5) showed that addition of water had a similar effect in this study. Weak bands at 1500 cm^{-1} and *ca.* 830 cm^{-1} suggests the presence of small amounts of CO_3^{2-} in the 0 vol% water material, with the spectrum dominated by the characteristic acetate bands at 1566, 1425 cm^{-1} and 618 cm^{-1}. As previously discussed the small amount of carbonate present is formed from water in the acetate precursor reacting with CO_2 to form carbonic acid. The materials prepared using 5, 10 and 15 vol% water co-solvent showed more dominant CO_3^{2-} bands, indicating significant carbonate contribution in the precipitates. It was noted that the band at 830 cm^{-1} in the material prepared with 15 vol% water co-solvent shifts towards 839 cm^{-1} in the materials prepared with less water co-solvent, indicating a change in the co-ordination of CO_3^{2-}. A sharp band at 863 cm^{-1} was visible only in the material prepared with 15 vol% water co-solvent, indicating an additional carbonate species was present, although this was not detected by XRD.

All the SAS precipitated materials showed weight loss below 150 °C during TGA, indicating retention of solvent from the SAS process (Fig. 6). Excluding the solvent desorption at <150 °C, materials prepared using 5, 10 and 15 vol% water co-solvent had weight losses of *ca.* 19, 18 and 21% respectively. This is very close to the theoretical

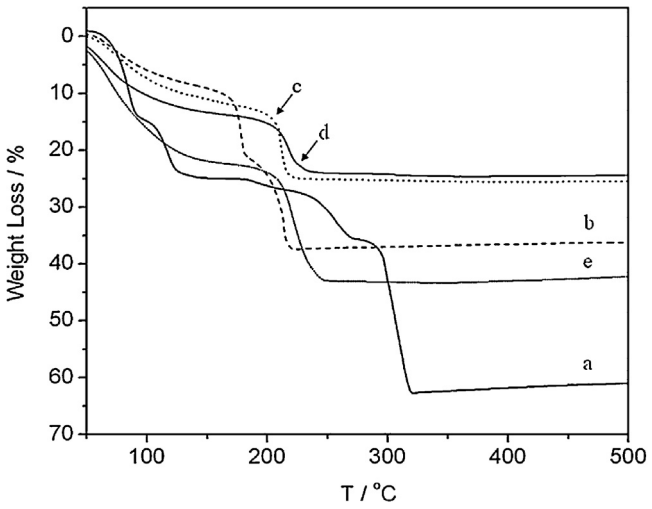

Fig. 6. TGA of cobalt SAS precipitates with different water co-solvent addition. (a) Commercial cobalt(II) acetate tetrahydrate, (b) 0 vol% water SAS, (c) 5 vol% water SAS, (d) 10 vol% water SAS, (e) 15 vol% water SAS.

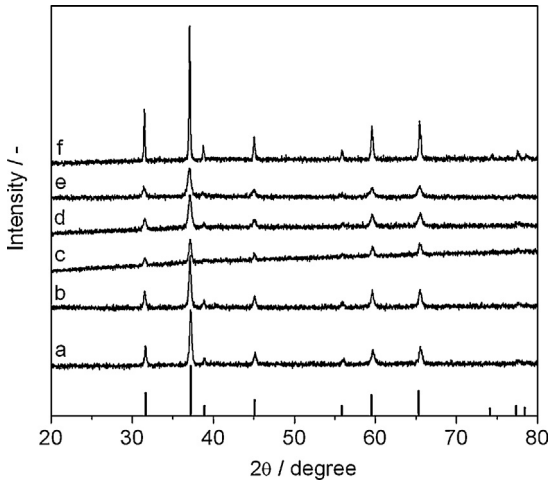

Fig. 7. XRD analysis of calcined cobalt SAS precipitates with different water co-solvent addition. Bars at the bottom indicate reflections of spinel Co_3O_4. (a) Commercial Co_3O_4, (b) calcined cobalt(II) acetate tetrahydrate, (c) 0 vol% water SAS, (d) 5 vol% water SAS, (e) 10 vol% water SAS, (f) 15 vol% water SAS.

weight loss expected for the decomposition of $Co(OH)_x(CO_3)_y{\cdot}H_2O$ to Co_3O_4 [40]. The weight loss of the material prepared without additional water was found to be *ca.* 29% and the decomposition profile was comparable to that expected for cobalt(II) acetate [41]. However, the weight loss (29%) was far from that expected for the decomposition of $Co(CH_3COO)_2$ to Co_3O_4 which should be 54%. The lower observed value indicates non-stoichiometric precipitation of a highly defective cobalt acetate material. The disordered and defective nature of these precipitated materials was further highlighted by the lack of any observable long range order from XRD analysis (not shown), as previously observed in other SAS precipitated materials [25,33]. The lower than expected weight loss for cobalt acetate, could also be due to the presence of some other cobalt species in the material. Species like cobalt hydroxides could be possible and their presence would be consistent with the lower weight loss. If such species were amorphous or had small crystallite sizes they would not be detected by XRD analysis.

The surface areas of the materials before and after calcination are given in Table 2. The surface area of material prepared with no additional water was noted to be substantially higher than the non-processed cobalt acetate, due to the high nucleation rates in SAS precipitation. As noted in previous studies [25], and in the metal acetate screening (Table 1), calcination resulted in a dramatic reduction of surface area. The addition of 5 vol% water resulted in a very similar trend to the water free prepared material, with the high precursor surface area reducing significantly after calcination. Higher levels of added water resulted in lower surface areas of the precipitates, which can be attributed to higher carbonate contents. Although the surface areas of the samples prepared using 5 and 10 vol% water co-solvent did decrease after calcination, the extent to which they decreased was reduced, as the final catalysts had higher surface areas compared to those prepared with 0 and 5 vol% water co-solvent.

Calcination of the cobalt SAS materials at 400 °C resulted in the formation of the spinel structured Co_3O_4 (ICDD: 42-1467), as observed by XRD (Fig. 7). The crystallite sizes, determined from the Scherrer equation, of the calcined SAS precipitated and standard materials are shown in Table 2. The 0 and 5 vol% water co-solvent derived catalysts were more crystalline, with crystallite sizes of *ca.* 40 nm, compared to the *ca.* 20 nm crystallites observed for catalysts prepared with 10 and 15 vol% water. The trend of crystallite size was directly comparable to the surface areas of the calcined catalysts, with smaller crystallites giving higher surface areas. Interestingly, the 0 and 5 vol% water co-solvent derived catalysts had comparable crystallite size to the standard calcined cobalt acetate salts. Therefore, it was evident that the precursor anion strongly influenced the resulting surface area and crystallite size of Co_3O_4. The acetate based precursors produced large crystallites due to the exothermic decomposition of metal acetates [35]. The carbonate rich precursors, observed in catalysts prepared with 10 and 15 vol% water, yielded relatively small crystallites and a limited reduction of surface area [36]. With regard to the catalyst prepared with 5 vol% water, carbonates were observed by FT-IR but the calcined material had crystallite sizes comparable to the metal acetate derived Co_3O_4. In addition to this, the extent of the decrease of surface area on calcination was more comparable to the metal acetate precursors. This suggests that whilst metal carbonate was clearly present in the catalyst prepared with 5 vol% water, there was a significant amount of acetate remaining.

TPR analysis was performed on Co_3O_4 catalysts derived from the materials precipitated using different concentrations of water co-solvent (Fig. 8). In addition, analysis was performed on a commercial Co_3O_4 sample, which showed a reduction peak at 385 °C, with a lower temperature shoulder at *ca.* 355 °C. This correlates

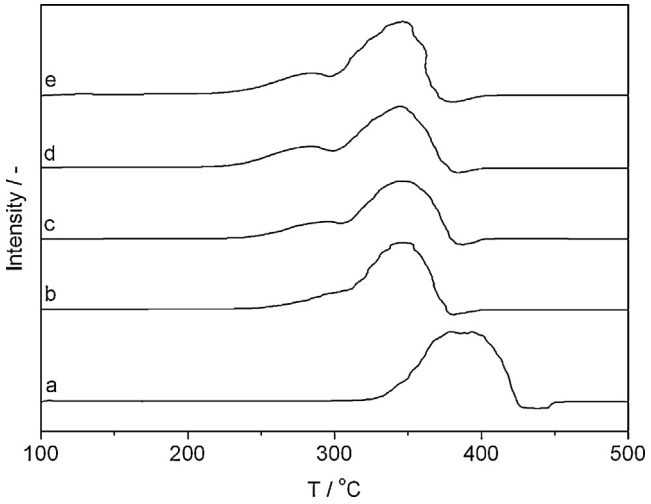

Fig. 8. TPR of calcined cobalt SAS precipitates with different water co-solvent addition. (a) Commercial Co_3O_4, (b) 0 vol% water SAS, (c) 5 vol% water SAS, (d) 10 vol% water SAS, (e) 15 vol% water SAS.

Table 2
Physical properties of Co SAS and standard precursors and catalysts calcined at 400 °C with corresponding catalytic performance for propane total oxidation. SAS preparation used between 0 and 15 vol% water as co-solvent.

	Surface area ($m^2\ g^{-1}$)		Crystallite size[a] (nm)	Catalytic activity[b] (°C)		Rate[c] ($mmol\ min^{-1}\ m^{-2}$)
	Precipitated	Calcined		T_{10}	T_{50}	
SAS 0% water	119	16	43	215	265	1.23×10^{-2}
SAS 5% water	131	15	41	200	230	2.84×10^{-2}
SAS 10% water	81	32	26	200	230	1.41×10^{-2}
SAS 15% water	54	35	24	155	240	9.28×10^{-3}
Cobalt acetate	8	2	45	250	305	8.40^{-3}
Co_3O_4	1	–	190	280	375	–

[a] Crystallite size calculated using Scherrer equation.
[b] Comparison of catalytic activity was determined by measuring the required temperature for 10 and 50% conversion.
[c] Rate of propane oxidation at 250 °C normalised for catalyst surface area.

with the expected reduction of Co_3O_4 to CoO and finally to Co. The SAS derived material profiles also had this two step reduction, although the reduction temperatures were lower than for the commercial Co_3O_4, with the CoO reduction peaks all being centred at *ca.* 350 °C. Interestingly the temperature of the first reduction step (Co_3O_4 to CoO) was more sensitive to the catalyst preparation conditions. The highest temperature for this reduction step, excluding the commercial Co_3O_4, was seen for the material precipitated without additional water at *ca.* 300 °C. The temperature then decreased with increasing water content in the SAS preparation up to 10 vol% water, after which it remains constant. The Co_3O_4 to CoO reduction temperature correlates directly with the Co_3O_4 crystallite sizes, with smaller crystallites giving lower Co_3O_4 to CoO reduction temperatures. It has previously been stated that lower initial temperatures of reduction indicate ease of mobility of oxygen in the oxide structure [7].

Representative SEM images of the precursors are shown in Fig. 9. The catalyst precursor prepared without water co-solvent comprised agglomerated semi-spherical nanoparticles. In the precursors prepared using 5 and 10 vol% water, spherical microparticles together with agglomerated semi-spherical nanoparticles were observed. With 15 vol% water, agglomerated material with some residual microspheres was observed. This change in morphology with respect to water content is highly indicative of a change in precipitation mechanism. The precipitation in the water free preparation would have been in a single phase system, well above the mixture critical point of CO_2–CH_3OH under the operating conditions of 120 bar and 40 °C [42]. The precipitation mechanism under these conditions is referred to being "gas like" with no surface tension, resulting in sub 100 nm semi-spherical particles [33]. The addition of water modifies the precipitation media by reducing the miscibility of CO_2 and the metal salt solution. This reduction in miscibility results in the presence of surface tension during the precipitation which stabilises the solution as droplets. The precipitation mechanism then requires CO_2 diffusion into a solution droplet to facilitate precipitation, which results in the formation of micron-scale spherical secondary morphologies, as observed in the SEM of samples produced with 5 and 10 vol% water co-solvent. Non-spherical morphologies were also observed in the water containing systems, which was attributed to the presence of a 2-phase system where a methanol rich phase resulted in the gas-like precipitation mechanism.

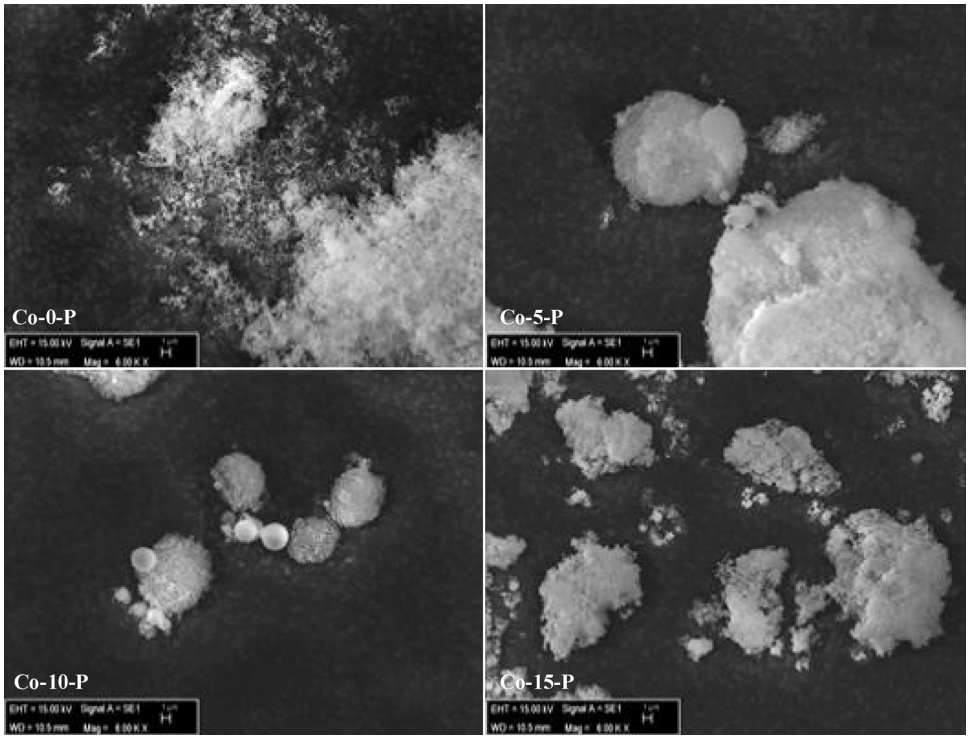

Fig. 9. SEM micrographs of cobalt SAS precipitates with different water co-solvent addition: 0 vol% water SAS (Co-0-P), 5 vol% water SAS (Co-5-P), 10 vol% water SAS (Co-10-P), 15 vol% water SAS (Co-15-P).

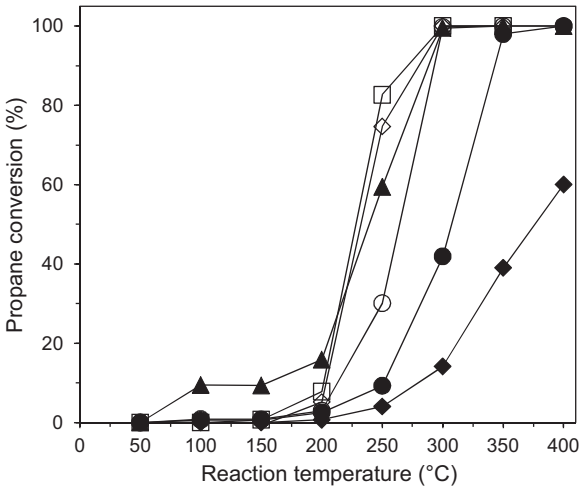

Fig. 10. Propane conversion as a function of temperature over various cobalt SAS precipitates with different water co-solvent. (○) 0 vol% water, (◊) 5 vol% water, (□) 10 vol% water, (▲) 15 vol% water, (♦) commercial Co_3O_4, (●) calcined cobalt(II) acetate tetrahydrate.

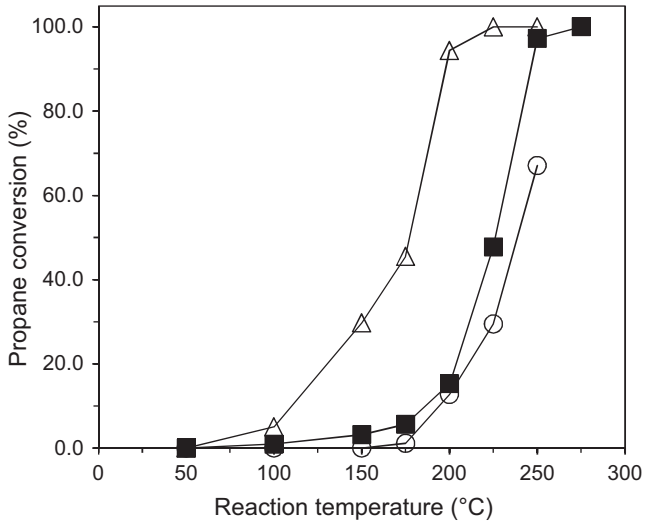

Fig. 11. Propane conversion as a function of temperature over catalysts derived from 5 and 10% water co-solvent SAS materials calcined at 250 °C, and 5 wt% Pt/Al_2O_3. (■) SAS 5 vol% water derived catalyst, (△) SAS 10 vol% water derived catalyst, (◯) 5 wt% Pt/Al_2O_3.

Light-off curves for the SAS prepared and standard Co_3O_4 catalysts are shown in Fig. 10, with T_{10} and T_{50} values given in Table 2. Interestingly, all of the SAS derived materials prepared with water as co-solvent converted 10% of propane at reaction temperatures <200 °C, with conversion being observed at temperatures as low as 50 °C and total combustion achieved at relatively low temperatures of 250–300 °C. The catalyst prepared without additional water required higher temperatures, around 350 °C, to fully oxidise the propane, with the standard cobalt acetate derived catalyst and the commercial Co_3O_4 requiring temperatures greater than 400 °C. From these data it was apparent that all of the SAS precipitated catalysts with water as co-solvent had comparable activity for propane oxidation. The lower T_{50} values for the 5 vol% water and the 10 vol% water SAS derived catalysts could be taken as evidence of enhanced activity, although the difference between these values and that of the catalyst produced with 15 vol% water co-solvent was only 20 °C, making this assertion tentative, due to potential experimental errors (*ca.* ±20 °C). The surface area normalised rates of propane oxidation are presented in Table 2. All of the SAS prepared Co_3O_4 catalysts showed rates greater than the Co_3O_4 prepared by calcination of the acetate, indicating that supercritical precipitation resulted in more active Co_3O_4 surfaces. Adding 5 vol% water significantly increased the normalised rate for Co3O4 when compared to precipitation with out water. The rate was greatest for the 5 vol% catalyst, whilst adding 10 and 15 vol% water resulted in successive reductions of the normalised rates.

It is clear that the commercial Co_3O_4 material, with substantially lower surface area, high crystallinity and poor reducibility was considerably less active than the other catalysts. Similar properties also resulted in the reduced activity of the SAS 0 vol% water co-solvent catalyst with a very low surface area. However, the correlation between the characteristic properties of the other catalysts and their activity was not so apparent, as differences in catalyst properties appeared to have negligible influence on catalyst performance. This was most apparent when comparing catalysts prepared using 5 and 10 vol% water co-solvent. Although activity was similar the latter had twice the surface area, much smaller crystallites and it also had a lower reduction temperature for the transition of Co_3O_4 to CoO. However, previous studies that have shown enhanced activity by altering catalyst properties have done so with far more substantial changes in such properties. For example Solsona et al. demonstrated enhanced activity of mechano-chemically prepared Co_3O_4 by increasing the surface area by a factor of five [6]. Evidently the variations in the SAS water co-solvent catalysts were not substantial enough to have a demonstrable effect on activity for propane total oxidation.

3.3. Investigation of the calcination treatment of Co precursors

TGA of the various Co precursor materials (Fig. 6) showed that the SAS derived materials had all fully decomposed by 250 °C. Further heat treatment to 400 °C was thought to result in coalescence of particles and so reduce differences between the materials imparted by variations in the SAS process. Hence the SAS materials prepared with 5 and 10 vol% water co-solvent were also calcined at 250 °C. The materials were shown to be Co_3O_4 by XRD, although lowering of calcination temperature from 400 °C to 250 °C reduced the crystallite size and increased the surface area of both materials (Table 3). The reduced calcination temperature was noted to have a greater effect on the properties of the catalyst made using 10 vol% water co-solvent. The surface area of 96 $m^2\ g^{-1}$, after 250 °C calcination, was comparable to that seen in the literature for very active catalysts [7–9]. The smaller improvement in surface area of the 5 vol% water co-solvent material was explained by the presence of higher quantities of acetate in the precursor. This is due to the exothermic nature of the acetate decomposition offsetting the effect of lowering the calcination temperature.

Unlike the catalysts calcined at 400 °C, the light off curves of the 5 and 10 vol% water co-solvent catalysts calcined at lower temperature show significantly different activities (Fig. 11). T_{50} and T_{10} values of the two catalysts are separated by 50 and 75 °C respectively (Table 3). The activity of the 5 vol% water co-solvent catalyst did not significantly change when the calcination temperature was decreased to 250 from 400 °C, whereas activity substantially improved with lower calcination temperature for the 10 vol% water co-solvent catalyst. The lack of activity improvement, for the lower calcination temperature of the 5 vol% water co-solvent catalyst, was expected when taking the materials physical properties into account. Whilst the surface area of the 5 vol% water co-solvent catalyst calcined at 250 °C increased and the crystallite size decreased, relative to the material calcined at 400 °C, the improvement resulted in properties similar to the 10 vol% water co-solvent catalyst calcined at 400 °C.

The requirement of a dramatic increase in surface area to enhance the activity has been previously noted, with Solsona

Table 3
Physical properties of Co SAS catalysts, prepared using 5 and 10% water co-solvent, calcined at 250 °C, with corresponding catalytic properties for total oxidation of propane. Values in parentheses show properties of corresponding catalysts calcined at 400 °C.

	Surface area ($m^2\ g^{-1}$)	Crystallite size[a] (nm)	Catalytic activity[b] (°C)	
			T_{10}	T_{50}
SAS 5% water	36 (15)	28 (41)	185 (200)	225 (230)
SAS 10% water	96 (32)	8 (26)	110 (200)	175 (230)

[a] Crystallite size calculated using Scherrer equation.
[b] Comparison of catalytic activity was determined by measuring the required temperature for 10 and 50% conversion.

et al. and Garcia et al. both reporting a non-linear relationship between activity and surface area [7,14]. The T_{10} and T_{50} values for catalyst prepared by SAS with 10 vol% water co-solvent and calcined at 250 °C are comparable with the highest reported for a bulk Co_3O_4 catalyst, which had T_{10} and T_{50} values of 145 and 165 °C respectively [6].

The best catalyst was Co_3O_4, derived from SAS precipitated cobalt acetate with 10 vol% water co-solvent and calcined under static air at 250 °C. Fig. 11 also provides a comparison of the catalyst performance with a commercial 5 wt% Pt/Al_2O_3 catalyst [43]. The precious metal catalyst is well known to be a highly effective total oxidation catalyst and consequently provides a bench mark for potential new catalysts. Evidently, while a standard crystalline Co_3O_4 has poor activity; SAS precipitated nanocrystalline Co_3O_4 is more active than the commercial 5 wt% Pt/Al_2O_3 catalyst. The performance of the SAS prepared catalyst was also studied with time-on-line, as some cobalt oxide catalysts have shown some degree of deactivation for hydrocarbon total oxidation. Over a preliminary test period of 30 h there was no deterioration of propane conversion, and additionally the catalyst did not show any deactivation when the temperature was cycled from ambient to temperatures giving 100% propane conversion.

4. Conclusions

We have demonstrated that several different transition metal oxides, namely Fe_3O_4, NiO, CuO and Co_3O_4, can be prepared using SAS precipitation. Co_3O_4 materials were found to be the most active catalysts for propane total oxidation, as noted in previous studies of conventionally prepared metal oxides [7–9]. The SAS precipitated Co_3O_4 material prepared during the initial screening showed comparable properties and activity to some mechano-chemically prepared materials, a technique that has been optimised to give higher surface areas and activities. The potential of the SAS Co_3O_4 catalyst resulted in further studies aimed towards further improving activity.

The addition of water co-solvent into the SAS process changed the precipitation environment resulting in a change in particle morphology and the formation of cobalt carbonates. These materials had residual acetate present, which reduced with increased amounts of water. Catalysts produced using 0 and 5 vol% water co-solvent calcined at 400 °C, had very similar properties in terms of surface area and crystallite size. The low surface areas and large crystallite sizes were attributed to the exothermic decomposition of cobalt acetate. On calcination catalysts prepared with 10 and 15 vol% water co-solvent had higher surface areas, due to the greater presence of carbonates. Reducibility of Co_3O_4 to CoO was also noted to increase slightly with an increase in water co-solvent in the SAS process. For catalysts calcined at 400 °C the variations in the physical properties of the catalysts had little impact on the activity, but it was established that the water co-solvent SAS precipitated catalysts were more active than the standard materials and the SAS precipitation without water.

Lowering the calcination temperature from 400 °C to 250 °C for SAS prepared materials with 5 and 10 vol% water co-solvent resulted in smaller crystallite sizes and increased surface areas. This was far more profound for the catalyst prepared with 10 vol% water and coincided with a significant improvement in catalytic activity. The observed temperatures of propane combustion for this catalyst were comparable to the most active mechano-chemically prepared catalyst, with considerably higher activity than a commercial precious metal 5 wt% Pt/Al_2O_3 catalyst, demonstrating that a novel, nitrate free and green supercritical anti-solvent precipitation process can successfully produce highly active short chain alkane total oxidation catalysts.

Acknowledgement

We gratefully acknowledge funding for this work from the UK Technology Strategy Board and we would like to thank Johnson Matthey for their involvement in the work.

References

[1] B.J. Finlayson-Pitts, J.N. Pitts, Science 276 (1997) 1045–1051.
[2] M.J. Molina, F.S. Rowland, Nature 249 (1974) 810–812.
[3] H. Rodhe, Science 248 (1990) 1217–1219.
[4] A. O'Malley, B.K. Hodnett, Catalysis Today 54 (1999) 31–38.
[5] T. Davies, T. Garcia, B. Solsona, S.H. Taylor, Chemical Communications 32 (2006) 3417–3419.
[6] B. Solsona, I. Vázquez, T. Garcia, T. Davies, S. Taylor, Catalysis Letters 116 (2007) 116–121.
[7] B. Solsona, T.E. Davies, T. Garcia, I. Vázquez, A. Dejoz, S.H. Taylor, Applied Catalysis B: Environmental 84 (2008) 176–184.
[8] M. Baldi, V.S. Escribano, J.M.G. Amores, F. Milella, G. Busca, Applied Catalysis B: Environmental 17 (1998) 175–182.
[9] M.R. Morales, B.P. Barbero, L.E. Cadús, Applied Catalysis B: Environmental 67 (2006) 229–236.
[10] M.R. Morales, B.P. Barbero, L.E. Cadús, Applied Catalysis B: Environmental 74 (2007) 1–10.
[11] B. Solsona, T. Garcia, S. Agouram, G.J. Hutchings, S.H. Taylor, Applied Catalysis B: Environmental 101 (2011) 388–396.
[12] Q. Liu, L.-C. Wang, M. Chen, Y. Cao, H.-Y. He, K.-N. Fan, Journal of Catalysis 263 (2009) 104–113.
[13] C. He, M. Paulus, W. Chu, J. Find, J.A. Nickl, K. Köhler, Catalysis Today 29 (2008) 305–313.
[14] T. Garcia, S. Agouram, J.F. Sánchez-Royo, R. Murillo, A.M. Mastral, A. Aranda, I. Vázquez, A. Dejoz, B. Solsona, Applied Catalysis A: General 386 (2010) 16–27.
[15] D.J. Dixon, G. Luna-Bárcenas, K.P. Johnston, Polymer 35 (1994) 3998–4005.
[16] A. O'Neil, C. Wilson, J.M. Webster, F.J. Allison, J.A.K. Howard, M. Poliakoff, Angewandte Chemie International Edition 41 (2002) 3796–3799.
[17] C.N. Field, P.A. Hamley, J.M. Webster, D.H. Gregory, J.J. Titman, M. Poliakoff, Journal of the American Chemical Society 122 (2000) 2480–2488.
[18] E. Reverchon, G.D. Porta, D. Sannino, L. Lisi, P. Ciambelli, Studies in Surface Science and Catalysis 118 (1998) 349–358.
[19] E. Reverchon, G. Della Porta, Powder Technology 106 (1999) 23–29.
[20] E. Reverchon, I. De Marco, G. Della Porta, Journal of Supercritical Fluids 23 (2002) 81–87.
[21] P.J. Miedziak, Z. Tang, T.E. Davies, D.I. Enache, J.K. Bartley, A.F. Carley, A.A. Herzing, C.J. Kiely, S.H. Taylor, G.J. Hutchings, Journal of Materials Chemistry 19 (2009) 8619–8627.
[22] Z.-R. Tang, J.K. Edwards, J.K. Bartley, S.H. Taylor, A.F. Carley, A.A. Herzing, C.J. Kiely, G.J. Hutchings, Journal of Catalysis 249 (2007) 208–219.
[23] G.J. Hutchings, J.K. Bartley, J.M. Webster, J.A. Lopez-Sanchez, D.J. Gilbert, C.J. Kiely, A.F. Carley, S.M. Howdle, S. Sajip, S. Caldarelli, C. Rhodes, J.C. Volta, M. Poliakoff, Journal of Catalysis 197 (2001) 232–235.
[24] G.J. Hutchings, J.A. Lopez-Sanchez, J.K. Bartley, J.M. Webster, A. Burrows, C.J. Kiely, A.F. Carley, C. Rhodes, M. Hävecker, A. Knop-Gericke, R.W. Mayer, R. Schlögl, J.C. Volta, M. Poliakoff, Journal of Catalysis 208 (2002) 197–210.

[25] Z.-R. Tang, C. Jones, J.W. Aldridge, T.E. Davies, J.K. Bartley, A.F. Carley, S.H. Taylor, M. Allix, C. Dickinson, M.J. Rosseinsky, J.B. Claridge, Z. Xu, M.J. Crudace, G.J. Hutchings, ChemCatChem 1 (2009) 247–251.
[26] C. Jones, K.J. Cole, S.H. Taylor, M.J. Crudace, G.J. Hutchings, Journal of Molecular Catalysis A: Chemical 305 (2009) 121–124.
[27] Z.R. Tang, S.A. Kondrat, C. Dickinson, J.K. Bartley, A.F. Carley, S.H. Taylor, T.E. Davies, M. Allix, M.J. Rosseinsky, J.B. Claridge, Z. Xu, S. Romani, M.J. Crudace, G.J. Hutchings, Catalysis Science & Technology 1 (2011) 740–746.
[28] P.T. Anastas, L.G. Williamson, Green Chemical Syntheses and Processes, American Chemical Society, Washington, DC, 2000.
[29] R. Noyori, Chemical Communications (2005) 1807–1811.
[30] E.J. Beckman, Journal of Supercritical Fluids 28 (2004) 121–191.
[31] E.J. Beckman, Industrial and Engineering Chemistry Research 42 (2003) 1598–1602.
[32] R. Adami, E. Reverchon, E. Järvenpää, R. Huopalahti, Powder Technology 182 (2008) 105–112.
[33] E. Reverchon, I. De Marco, E. Torino, Journal of Supercritical Fluids 43 (2007) 126–138.
[34] E. Reverchon, G. Della Porta, D. Sannino, P. Ciambelli, Powder Technology 102 (1999) 127–134.
[35] T. Wanjun, C. Donghua, Chemical Papers 61 (2007) 329–332.
[36] P. Porta, G. Moretti, M. Musicanti, A. Nardella, Catalysis Today 9 (1991) 211–218.
[37] C.-W. Tang, C.-B. Wang, S.-H. Chien, Thermochimica Acta 473 (2008) 68–73.
[38] L. Christel, A. Pierre, D.A.R. Abel, Thermochimica Acta 306 (1997) 51–59.
[39] M. Liang, W. Kang, K. Xie, Journal of Natural Gas Chemistry 18 (2009) 110–113.
[40] R. Xu, H.C. Zeng, Journal of Physical Chemistry B 107 (2003) 12643–12649.
[41] Z. Nickolov, G. Georgiev, D. Stoilova, I. Ivanov, Journal of Molecular Structure 354 (1995) 119–125.
[42] J.W. Ziegler, J.G. Dorsey, Analytical Chemistry 67 (1995) 456–461.
[43] J.J. Spivey, Industrial and Engineering Chemistry Research 26 (1987) 2165–2180.